J Solution Chem
DOI 10.1007/s10953-016-0486-6

Molecular Docking, Potentiometric and Thermodynamic Studies of Some Azo Compounds

A. A. El-Bindary[1] · M. M. Ghoneim[2] · M. A. Diab[1] · A. Z. El-Sonbati[1] · A. F. Shoair[1] · M. K. Abd El-Kader[1]

Received: 28 November 2015 / Accepted: 26 April 2016
© Springer Science+Business Media New York 2016

Abstract The proton-ligand dissociation constant of 5-(4′-alkylphenylazo)-3-phenylamino-2-thioxothiazolidin-4-one (**HL$_n$**) ($n = 1$, R = –CH_3; $n = 2$, –H and $n = 3$, –Cl) and metal–ligand stability constants of its complexes with metal ions (Mn^{2+}, Co^{2+}, Ni^{2+} and Cu^{2+}) have been determined potentiometrically in 0.1 mol·dm^{-3} KCl and 40 % (by volume) DMF–water mixture and at 298, 308 and 318 K. The stability constants of the formed complexes increase with the order $Mn^{2+} < Co^{2+} < Ni^{2+} < Cu^{2+}$. The effect of temperature was studied and the corresponding thermodynamic parameters ($\Delta G°$, $\Delta H°$ and $\Delta S°$) were derived and discussed. The dissociation process of the ligands is endothermic and entropically unfavorable. The formation of the metal complexes has been found to be endothermic and entropically favorable. Molecular docking was used to predict the binding mode between azo rhodanine derivatives (**HL$_n$**) with the 3hb5-oxidoreductase receptor of breast cancer. The values of binding constants (K_i) of the azo rhodanine derivatives (**HL$_n$**) are correlated with Hammett's constant (σ^R).

Keywords Azo rhodanine · Potentiometry · Thermodynamics · Molecular docking

1 Introduction

The formation of complexes in aqueous solutions is a matter of great importance not only in inorganic and analytical chemistry, biochemistry and other scientific and industrial fields [1, 2]. Azo rhodanine and its derivatives have wide industrial applications as intermediates in the synthesis of dyes, antioxidants and brightening additives in silver electroplating, as well as pharmacological [3], and biological activities [4–6]. Another interesting aspect of

✉ A. A. El-Bindary
abindary@yahoo.com

[1] Department of Chemistry, Faculty of Science, Damietta University, Damietta 34517, Egypt

[2] Department of Chemistry, Faculty of Science, Tanta University, Tanta, Egypt

Published online: 17 June 2016

the chemistry of these compounds is their donating power to metal ions, which makes them strong ligands in coordination compounds [7, 8]. These compounds are also used in analytical chemistry as highly sensitive reagents for heavy metals [9, 10]. Many binary complexes of transition and inner transition metals have been studied potentiometrically [11, 12]. Metal complexes of rhodanine have been extensively studied because rhodanine possess good synthetic flexibility, selectivity and sensitivity towards the central metal atom [13–15].

Breast cancer now represents the most common female malignancy in both the developing and developed world, and is the primary cause of death among women globally [16]. Cancer can be described as the uncontrolled growth of abnormal cells. At the global level, it accounted for more than 1.6 million new cases in 2010. The incidence or prevalence rate of the breast cancer in India is expected to be more than 90,000 in the coming years and over 50,000 women die each year.

In the present paper, we describe the dissociation constant of azo rhodanine derivatives ($\mathbf{HL}_n$) and the stability constants for its complexes with Mn^{2+}, Co^{2+}, Ni^{2+} and Cu^{2+}, which were obtained by potentiometric studies. Also, the corresponding thermodynamic functions of the dissociation and stability constants are derived and discussed. Also, we discuss the binding ability of azo rhodanine derivatives ($\mathbf{HL}_n$) with the 3hb5-oxidoreductase receptor of breast cancer.

2 Experimental

2.1 Measurements

Elemental microanalyses of the separated ligands for C, H, and N were determined on an Automatic Analyzer CHNS Vario ELIII (Germany). The ^{1}H NMR spectra was obtained by a Bruker WP 300 MHz using DMSO–d_6 as a solvent containing TMS as the internal standard. IR spectra (KBr discs, 4000–400 cm^{-1}) were measured by a Jasco-4100 spectrophotometer. Mass spectrum was recorded by the EI technique at 70 eV using a MS-5988 GS–MS (Hewlett–Packard). The pH measurements were carried out using VWR Scientific Instruments Model 8000 pH-meter accurate to ±0.01 units. The pH–meter readings in the non-aqueous medium were corrected [17]. The electrode system was calibrated according to the method of Irving et al. [18]. The temperature was controlled to within ± 0.05 K by circulating thermostated water (Neslab 2 RTE 220) through the outer jacket of the vessel. All titrations have been carried out between pH = 3.5 and 12.0, under nitrogen atmosphere.

The study simulates the actual docking process in which the ligand–protein pairwise interaction energies were calculated using Docking Server [19]. The MMFF94 force field was used for energy minimization of the ligand molecule using Docking Server. Gasteiger partial charges were added to the ligand atoms. Non-polar hydrogen atoms were merged, and rotatable bonds were defined. Docking calculations were carried out on a 3hb5–OXIDORDUCTASE–Hormone protein model. Essential hydrogen atoms, Kollman united atom type charges, and solvation parameters were added with the aid of AutoDock tools [20]. Affinity (grid) maps of 20 Å× 20 Å× 20 Å grid points and 0.375 Å spacing were generated using the Autogrid program [21]. AutoDock parameter set- and distance-dependent dielectric functions were used in the calculation of the van der Waals and the electrostatic terms, respectively.

2.2 Materials

All chemicals used in this investigation were chemically pure grade derived from BDH. They include chlorides of Mn^{2+}, Co^{2+}, Ni^{2+} and Cu^{2+}, sodium hydroxide (NaOH) (97 %), sodium nitrite ($NaNO_2$) (97 %), and hydrochloric acid (HCl) (37 %), purchased from BDH. The standard chemicals aniline (99 %) and 4-alkylanilines (alkyl: CH_3 (99 %) and Cl (98 %)) purchased from Aldrich, Fluka and Merck were used without any further purification. Water used was bidistilled water; the distillation process was carried out using both condensation process and ion exchange technique.

2.3 Preparation of Azo Rhodanine Derivatives

Preparation of 5-(4′-alkylphenylazo)-3-phenylamino-2-thioxothiazolidin-4-one (**HL_n**): in typical preparation, 25 mL of distilled water containing hydrochloric acid (12 mol·dm^{-3}, 2.68 mL, 32.19 mmol) was added to aniline (0.979 mL, 10.73 mmol) or a 4-alkyl-aniline. To the resulting mixture stirred and cooled to 273 K, a solution of sodium nitrite (740 mg, 10.73 mmol, in 20 mL of water) was added dropwise. The so-formed diazonium chloride was consecutively coupled with an alkaline solution of 3-phenylamino-2-thioxothiazolidin-4-one (10.73 mmol) in 20 mL of pyridine. The precipitate, which formed immediately, was filtered and washed several times with water. The crude products were purified by recrystallization from hot ethanol [22]. The elemental analyses data for ligands are given in Table 1.

The resulting formed ligands are:

HL_1 = 5-(4′-methylphenylazo)-3-phenylamino-2-thioxothiazolidin-4-one.

HL_2 = 5-(4′-phenylazo)-3-phenylamino-2-thioxothiazolidin-4-one.

HL_3 = 5-(4′-chlorophenylazo)-3-phenylamino-2-thioxothiazolidin-4-one.

2.4 pH Titration

The experimental procedure involved the titration of the following solutions (total volume = 50 mL) against a standard CO_2 free (0.002 mol·dm^{-3}) NaOH solution. The following mixtures (i)–(iii) were prepared and titrated potentiometrically at 298 K against standard 0.002 mol·dm^{-3} NaOH in a 40 % (by volume) DMF–water mixture:

(i) 5 cm^3 0.001 mol·dm^{-3} HCl + 5 cm^3 1 mol·dm^{-3} KCl + 20 cm^3 DMF.

(ii) 5 cm^3 0.001 mol·dm^{-3} HCl + 5 cm^3 1 mol·dm^{-3} KCl + 15 cm^3 DMF + 5 cm^3 0.00 1 mol·dm^{-3} ligand.

Table 1 Elemental analyses data of the ligands (**HL_n**)

Compound	% Exp. (calc.)		
	C	H	N
HL_1	56.0 (55.8)	4.1 (4.1)	16.4 (16.4)
HL_2	54.9 (54.8)	3.7 (3.6)	17.1 (16.9)
HL_3	49.7 (49.6)	3.1 (3.0)	15.5 (15.4)

(iii) 5 cm^3 0.001 $mol \cdot dm^{-3}$ HCl + 5 cm^3 1 $mol \cdot dm^{-3}$ KCl + 15 cm^3 DMF + 5 cm^3 0.001 $mol \cdot dm^{-3}$ ligand + 10 cm^3 0.0001 $mol \cdot dm^{-3}$ metal chloride.

For each mixture, the volume was made up to 50 cm^3 with bidistilled water before the titration. These titrations were repeated for temperatures of 308 K and 318 K.

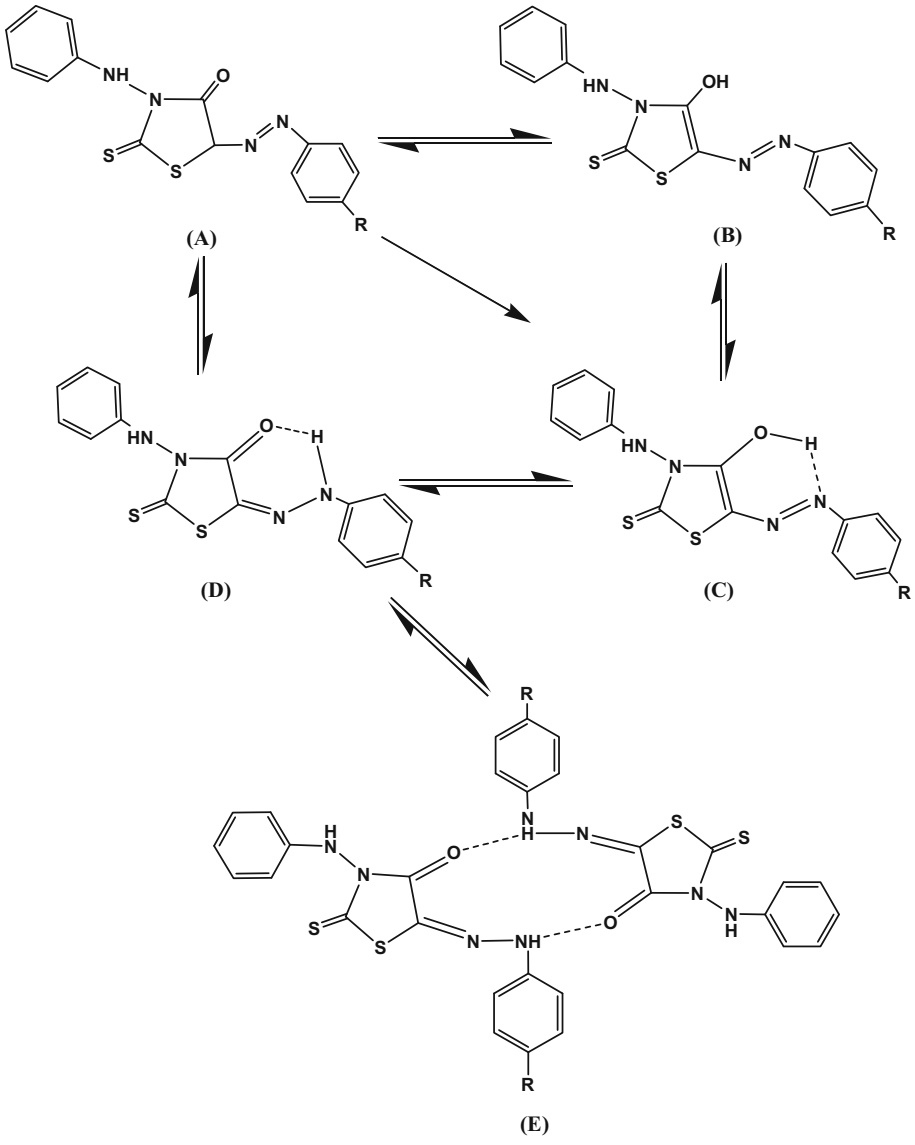

Fig. 1 Intramolecular and intermolecular hydrogen-bonded structure of 5-(4′-alkylphenylazo)-3-phenylamino-2-thioxothiazolidin-4-one (**HL**$_n$)

The ligands solutions (0.001 mol·dm^{-3}) were prepared by dissolving an accurately weighed amount of the solid in DMF. Metal ion solutions (0.0001 mol·dm^{-3}) were prepared from analar metal chlorides in bidistilled water and standardized with EDTA [23]. Solutions of 0.001 mol·dm^{-3} HCl and 1 mol·dm^{-3} KCl were also prepared in bidistilled water. A carbonate free sodium hydroxide solution in 40 % (by volume) DMF–water mixture was used as titrant and standardized against analar oxalic acid [24–27].

3 Results and Discussion

3.1 Structure of the Ligands

IR spectra provide valuable information regarding the nature of the functional group attached to the metal atom. The spectra of ligands do not show absorption characteristic of the N=N function owing to the formation of the hydrazone (Fig. 1). The ligand IR spectra give interesting results and conclusions; thus, the three bands around 823–882 and 3205–3210 cm^{-1} in the ligands are assigned to υ(CS) and –NH(3-phenylamine),

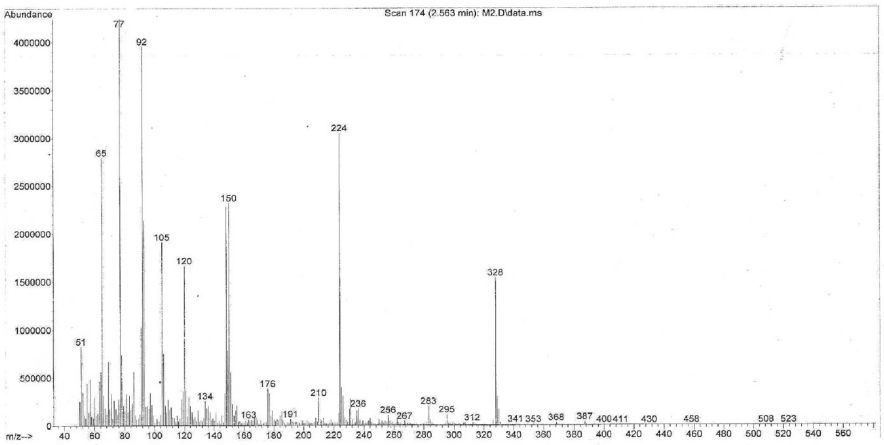

Fig. 2 **a** Mass spectrum and **b** fragmentation patterns of $\mathbf{HL_2}$ ligand

respectively. The splitting of the υ(N=N) band into two bands in the ranges 1435–1520 and $\sim$1230 cm^{-1} due to υ(HC=N) and υ(=N–NH) hydrazone, respectively, for ligands provides evidence that the hydrazone N participate in the chelation after deprotonation leading to a covalent linkage. The IR spectral data of the ligands (**HL_n**) exhibit a band at 1727–1754 cm^{-1} due to C=O [22]. There are broad bands, which can be attributed to different types of intramolecular hydrogen-bonded –NH groups (Fig. 1c, d) and intermolecular hydrogen bond (Fig. 1e).

The ^{1}H NMR spectra of the ligands were recorded in DMSO–d_6 solution using TMS as internal standard. The broad signal exhibited by the ligands can be assigned to an intramolecularly hydrogen bonded proton of NH (hydrazone)/OH (enol) at $\sim$11.5 ppm and NH (3-phenylamine) at $\sim$9.0 ppm, which were not affected by dilution and disappeared in the presence of D_2O. The aromatic rings give a group of multi-signals at 6.5–8.0 ppm. The singlet peak observed at 2.3 ppm can be assigned to the proton of the CH_3 group.

The mass spectrum fragmentation mode of ligand (**HL_2**) shows the exact mass of 328 corresponding to the formula $C_{15}H_{12}N_4OS_2$ as shown in Fig. 2a. The ion of $m/z = 328$ undergoes fragmentation to a stable peak at $m/z = 224$ by losing the $C_6H_5N_2$ (structure **I**) as shown in Fig. 2b. The loss of $C_3H_2N_2OS_2$ leads to the fragmentation with $m/z = 77$ (structure **II**).

3.2 Potentiometric and Thermodynamic Studies

From the titration curves of the acid in the absence and presence of ligands (**HL_n**), the average number of the protons associated with ligands (**HL_n**) at different pH values, $\bar{n}_A$, was calculated from Eq. 1:

$$\bar{n}_A = Y \pm \frac{(V_1 - V_2)(N^o + E^o)}{(V^o - V_1)TC_L^o} \quad (1)$$

where Y is the number of available protons in the ligand (**HL_n**) ($Y = 1$) and V_1 and V_2 are the volumes of alkali required to reach the same pH on the titration curve of hydrochloric

Table 2 Thermodynamic functions for the dissocation of ligands (**HL_n**) in 40 % (by volume) DMF–water mixtures and 0.1 $mol{\cdot}dm^{-3}$ KCl at different temperatures

Compound	Temperature (K)	Dissociation constant pK_1^H	Gibbs energy ($kJ{\cdot}mol^{-1}$) ΔG°	Enthalpy change ($kJ{\cdot}mol^{-1}$) ΔH°	Entropy change ($J{\cdot}mol^{-1}{\cdot}K^{-1}$) $-\Delta S^\circ$
HL_1	298	8.58 (±0.02)	48.96 (±0.11)		79 (±3)
	308	8.43 (±0.03)	49.71 (±0.17)	25 (±3)	79 (±3)
	318	8.30 (±0.05)	50.54 (±0.30)		79 (±3)
HL_2	298	8.37 (±0.04)	47.76 (±0.22)		72 (±2)
	308	8.21 (±0.03)	48.42 (±0.17)	26 (±2)	72 (±2)
	318	8.08 (±0.02)	49.20 (±0.12)		72 (±2)
HL_3	298	8.19 (±0.05)	46.73 (±0.28)		69 (±2)
	308	8.05 (±0.04)	47.47 (±0.23)	26 (±2)	69 (±2)
	318	7.90 (±0.03)	48.10 (±0.18)		69 (±2)

Table 3 Stepwise stability constants for complexes of ligand ($\mathbf{HL}_n$) in 40 % (by volume) DMF–water mixtures and 0.1 mol·dm^{-3} KCl at different temperatures

Compound	M^{n+}	298 K		308 K		318 K	
		$\log_{10} K_1$	$\log_{10} K_2$	$\log_{10} K_1$	$\log_{10} K_2$	$\log_{10} K_1$	$\log_{10} K_2$
$\mathbf{HL_1}$	Mn^{2+}	6.01 (±0.07)	4.28 (±0.05)	6.17 (±0.06)	4.40 (±0.06)	6.33 (±0.05)	4.51 (±0.06)
	Co^{2+}	6.13 (±0.05)	4.41 (±0.06)	6.25 (±0.05)	4.55 (±0.07)	6.39 (±0.04)	4.67 (±0.07)
	Ni^{2+}	6.28 (±0.06)	4.52 (±0.05)	6.42 (±0.04)	4.65 (±0.08)	6.60 (±0.07)	4.77 (±0.08)
	Cu^{2+}	6.40 (±0.07)	4.65 (±0.07)	6.56 (±0.05)	4.78 (±0.04)	6.74 (±0.06)	4.89 (±0.07)
$\mathbf{HL_2}$	Mn^{2+}	6.23 (±0.06)	4.50 (±0.08)	6.36 (±0.06)	4.61 (±0.05)	6.47 (±0.05)	4.74 (±0.06)
	Co^{2+}	6.36 (±0.05)	4.62 (±0.04)	6.47 (±0.07)	4.74 (±0.08)	6.59 (±0.07)	4.85 (±0.07)
	Ni^{2+}	6.50 (±0.04)	4.75 (±0.05)	6.62 (±0.08)	4.86 (±0.07)	6.76 (±0.04)	4.99 (±0.06)
	Cu^{2+}	6.62 (±0.07)	4.83 (±0.06)	6.74 (±0.05)	4.95 (±0.06)	6.85 (±0.05)	5.08 (±0.05)
$\mathbf{HL_3}$	Mn^{2+}	6.49 (±0.06)	4.69 (±0.07)	6.61 (±0.07)	4.80 (±0.05)	6.74 (±0.07)	4.93 (±0.04)
	Co^{2+}	6.62 (±0.07)	4.80 (±0.05)	6.73 (±0.06)	4.93 (±0.04)	6.84 (±0.06)	5.05 (±0.06)
	Ni^{2+}	6.77 (±0.06)	4.93 (±0.07)	6.89 (±0.07)	5.07 (±0.05)	7.00 (±0.04)	5.19 (±0.08)
	Cu^{2+}	6.79 (±0.05)	5.05 (±0.08)	6.90 (±0.05)	5.19 (±0.06)	7.03 (±0.07)	5.31 (±0.07)

acid and reagent, respectively, V° is the initial volume (50 cm^3) of the mixture, TC^{o}_{L}, is the total concentration of the reagent, N° is the normality of the sodium hydroxide solution and E° is the initial concentration of the free acid. Thus, the formation curves ($\bar{n}_A$ against pH) for the proton–ligand systems were constructed and found to extend between 0 and 1 in the $\bar{n}_A$ scale. This means that ligands ($\mathbf{HL}_n$) have one ionizable proton (the enolized hydrogen ion of the –OH group, pK^H). The dissociation constants were evaluated by different computational methods [28]. Three replicate titrations were performed; the average values obtained for ligands $\mathbf{HL}_n$ are listed in Table 2. The completely protonated form of the ligands ($\mathbf{HL}_n$) has one proton that dissociates in the measurable pH range. The deprotonation of the enol group most probably results in the formation of stable intramolecular H–bonding with the nitrogen of the N=N group. Such an interaction increases the dissociation process of enolic OH group and decreases the pK^H value in the order $\mathbf{HL_1} > \mathbf{HL_2} > \mathbf{HL_3}$ [29, 30].

The formation curves for the metal complexes were obtained by plotting the average number of ligands attached per metal ion ($\bar{n}$) against the free ligands exponent (pL), according to Irving and Rossotti [31]. The average number of the reagent molecules attached per metal ion, $\bar{n}$, and free ligands exponent, pL, can be calculated using Eqs. 2 and 3:

$$\bar{n} = \frac{(V_3 - V_2)(N^{o} + E^{o})}{(V^{o} - V_2) \cdot \bar{n}_A \cdot TC^{o}_{M}} \tag{2}$$

and

$$\mathrm{pL} = \log_{10}\left\{ \frac{\sum_{n=o}^{n=J} \beta^{H}_{n} \left(\frac{1}{[H^+]}\right)^{n}}{TC^{o}_{L} - \bar{n} \cdot TC^{o}_{M}} \cdot \frac{V^{o} + V_3}{V^{o}} \right\} \tag{3}$$

where TC^{o}_{M} is the total concentration of the metal ion present in the solution, and β^{H}_{n} is the overall proton–reagent stability constant. V_1, V_2 and V_3 are the volumes of alkali required to reach the same pH on the titration curves of hydrochloric acid, organic ligand and complex, respectively. These curves were analyzed and the successive metal–ligand stability constants were determined using different computional methods [32, 33]. The values of the stability constants ($\log_{10} K_1$ and $\log_{10} K_2$) are given in Table 3. The following general remarks can be made:

(i) The maximum value of $\bar{n}$ is ~ 2 indicating the formation of 1:1 and 1:2 (metal: ligand) complexes [34].

(ii) The metal ion solution used in the present study was very dilute (2×10^{-5} mol·dm^{-3}), hence there was no possibility of formation of polynuclear complexes [35, 36].

(iii) The metal titration curves were displaced to the right-hand side of the ligand titration curves along the volume axis, indicating proton release upon complex formation of the metal ion with the ligand. The large decrease in pH for the metal titration curves relative to ligand titration curves points to the formation of strong metal complexes [37, 38].

(iv) For the same ligand at constant temperature, the stability of the chelates increases with the order $Mn^{2+} < Co^{2+} < Ni^{2+} < Cu^{2+}$ [39–41]. This order largely reflects the considerably greater the stability of Cu^{2+} complexes compared to those of

other metals of the 3d series. Under the influence of both the polarizing ability of the metal ion [42] and the ligand field [43], Cu^{2+} will receive some extra stabilization due to tetragonal distortion of octahedral symmetry in its complexes. The greater stability of Cu^{2+} complexes is produced by the well known Jahn–Teller effect [43].

The dissociation constant (pK^{H}) for ligands (**HL$_n$**), as well as the stability constants of its complexes with Mn^{2+}, Co^{2+}, Ni^{2+} and Cu^{2+} have been evaluated at 298, 308 and 318 K, and are given in Tables 2 and 3, respectively. The enthalpy (ΔH°) for the dissociation and complexation process was calculated from the slope of the plot pK^{H} or $\log_{10} K$ against T^{-1} (Fig. 3) using the graphical representation of van't Hoff, Eqs. 4 and 5:

$$\Delta G^{\circ} = -2.303\, RT \log_{10} K = \Delta H^{\circ} - T\,\Delta S^{\circ} \tag{4}$$

or

$$\log_{10} K = (-\Delta H^{\circ}/2.303R).(1/T) + (\Delta S^{\circ}/2.303R) \tag{5}$$

From the ΔG° and ΔH° values one can deduce the entropy ΔS° using the well known relationships 4 and 6:

$$\Delta S^{\circ} = (\Delta H^{\circ} - \Delta G^{\circ})/T \tag{6}$$

All thermodynamic parameters of the dissociation process of ligands (**HL$_n$**) are recorded in Table 2. From these results the following conclusions can be made:

(i) The pK^{H} values decrease with increasing temperature, i.e. the acidity of the ligand increases [20].
(ii) A positive value of ΔH° indicates that the process is endothermic.
(iii) A large positive value of ΔG° indicates that the standard state dissociation process is not spontaneous [44].
(iv) A negative value of ΔS° is obtained due to the increased order as a result of the solvation process.

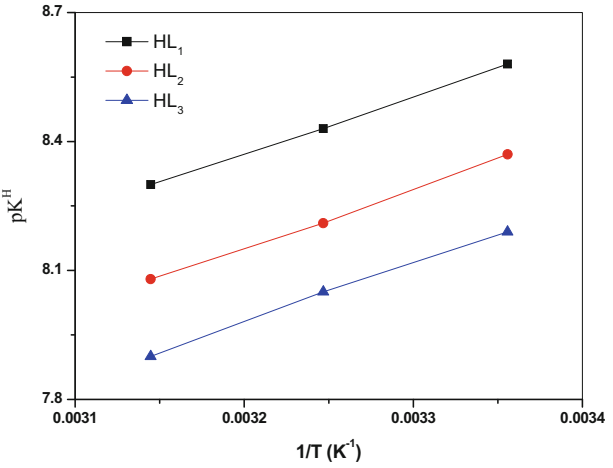

Fig. 3 van't Hoff plot pK^{H} of ligands (**HL$_n$**) against $1/T$

Table 4 Thermodynamic functions for ML_n complexes of ligand ($\mathbf{HL_n}$) in 40 % (by volume) DMF–water mixtures and 0.1 mol·dm^{-3} KCl

Compound	M^{n+}	T/K	Gibbs energy (kJ·mol^{-1})		Enthalpy change (kJ·mol^{-1})		Entropy change (J·mol^{-1}·K^{-1})	
			$-\Delta G_1^o$	$-\Delta G_2^o$	$-\Delta H_1^o$	$-\Delta H_2^o$	$-\Delta S_1^o$	$-\Delta S_2^o$
$\mathbf{HL_1}$	Mn^{2+}	298	34.29 (±0.39)	24.42 (±0.28)	29 (±2)	21 (±1)	212 (±2)	152 (±1)
		308	36.38 (±0.35)	25.94 (±0.35)			212 (±2)	152 (±1)
		318	38.54 (±0.30)	27.46 (±0.36)			212 (±2)	152 (±1)
	Co^{2+}	298	34.97 (±0.28)	25.16 (±0.34)	24 (±1)	24 (±1)	196 (±1)	164 (±1)
		308	36.85 (±0.29)	26.83 (±0.41)			196 (±1)	164 (±1)
		318	38.90 (±0.24)	28.43 (±0.42)			196 (±1)	164 (±1)
	Ni^{2+}	298	35.83 (±0.34)	25.79 (±0.28)	29 (±1)	23 (±3)	217 (±1)	163 (±3)
		308	37.86 (±0.23)	27.42 (±0.47)			217 (±1)	163 (±3)
		318	40.18 (±0.42)	29.04 (±0.48)			218 (±1)	163 (±3)
	Cu^{2+}	298	36.51 (±0.39)	26.53 (±0.39)	31 (±1)	22 (±1)	226 (±1)	162 (±1)
		308	38.68 (±0.29)	28.18 (±0.23)			226 (±1)	162 (±1)
		318	41.03 (±0.36)	29.77 (±0.42)			226 (±1)	162 (±1)
$\mathbf{HL_2}$	Mn^{2+}	298	35.54 (±0.34)	25.67 (±0.45)	22 (±1)	25 (±3)	192 (±1)	171 (±3)
		308	37.50 (±0.35)	27.18 (±0.29)			193 (±1)	171 (±3)
		318	39.39 (±0.30)	29.10 (±0.36)			192 (±1)	171 (±3)
	Co^{2+}	298	36.28 (±0.28)	26.36 (±0.22)	21 (±2)	21 (±3)	192 (±2)	158 (±3)
		308	38.15 (±0.41)	27.95 (±0.47)			192 (±2)	159 (±3)
		318	40.12 (±0.42)	29.53 (±0.42)			192 (±2)	158 (±3)
	Ni^{2+}	298	37.08 (±0.22)	27.10 (±0.28)	24 (±1)	22 (±1)	204 (±1)	164 (±1)
		308	39.04 (±0.47)	28.66 (±0.41)			203 (±1)	164 (±1)
		318	41.16 (±0.24)	30.38 (±0.36)			204 (±1)	164 (±1)
	Cu^{2+}	298	37.77 (±0.39)	27.55 (±0.34)	21 (±1)	23 (±1)	197 (±1)	169 (±1)
		308	39.74 (±0.29)	29.19 (±0.35)			197 (±1)	168 (±1)
		318	41.70 (±0.30)	30.93 (±0.30)			197 (±1)	169 (±1)
$\mathbf{HL_3}$	Mn^{2+}	298	37.03 (±0.34)	26.76 (±0.39)	23 (±1)	22 (±3)	200 (±1)	163 (±3)
		308	38.98 (±0.41)	28.30 (±0.29)			200 (±1)	163 (±3)
		318	41.03 (±0.42)	30.01 (±0.24)			200 (±1)	163 (±3)
	Co^{2+}	298	37.77 (±0.39)	27.38 (±0.34)	20 (±1)	23 (±1)	194 (±1)	168 (±1)
		308	39.68 (±0.35)	29.07 (±0.23)			194 (±1)	168 (±1)
		318	41.64 (±0.36)	30.74 (±0.36)			194 (±1)	168 (±1)
	Ni^{2+}	298	38.62 (±0.34)	28.12 (±0.39)	21 (±2)	24 (±1)	200 (±2)	174 (±1)
		308	40.63 (±0.41)	29.89 (±0.29)			200 (±2)	174 (±1)
		318	42.62 (±0.24)	31.60 (±0.48)			200 (±2)	174 (±1)
	Cu^{2+}	298	38.74 (±0.28)	28.81 (±0.45)	22 (±2)	24 (±1)	203 (±2)	176 (±1)
		308	40.69 (±0.29)	30.60 (±0.35)			203 (±2)	176 (±1)
		318	42.80 (±0.42)	32.33 (±0.42)			203 (±2)	176 (±1)

All the thermodynamic parameters of the stepwise stability constants of complexes are recorded in Table 4. The values of $\Delta H°$ and $\Delta S°$ can then be considered as the sum of two contributions: (a) release of H_2O molecules, and (b) metal–ligand bond formation. Examination of these values shows that:

(i) The stability constants ($\log_{10} K_1$ and $\log_{10} K_2$) for ligand (**HL$_n$**) complexes increase with increasing temperature, [45].

(ii) The negative value of $\Delta G°$ for the complexation process suggests the favorable nature of the standard state processes [46].

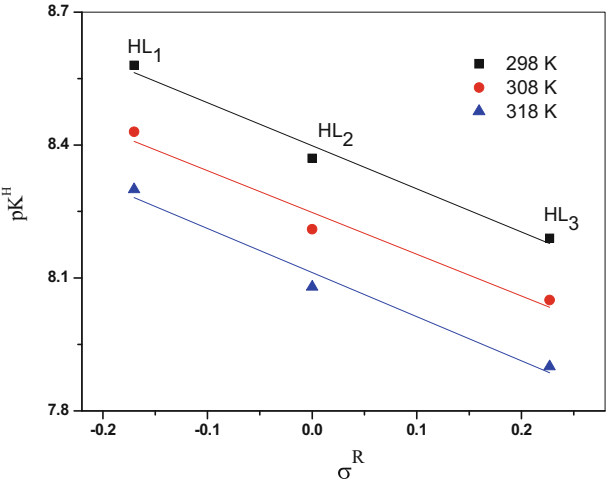

Fig. 4 Correlation of pK^H with Hammett's constant (σ^R) at 289, 308 and 310 K

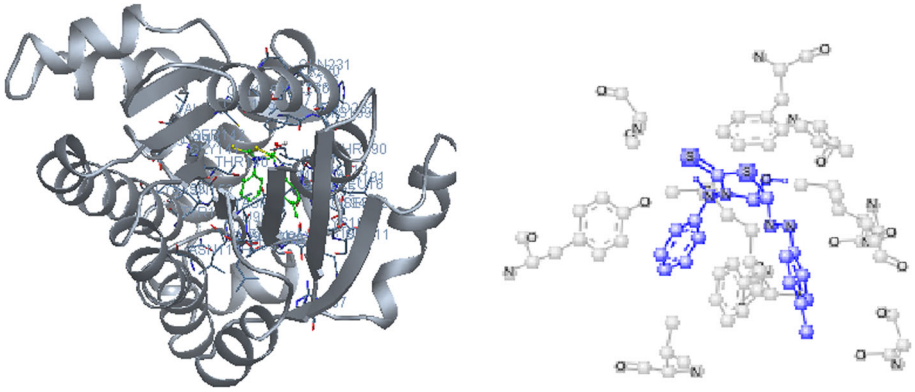

Fig. 5 The ligand (**HL$_1$**) [*green* in (**a**) and *blue* in (**b**)] in interaction with receptor breast cancer mutant 3hb5. (For interpretation of the references to color in this figure legend, the reader is referred to the web version of this article.) (Color figure online)

(iii) The $\Delta H°$ values are positive, meaning that these processes are endothermic and so more favorable at higher temperature.

(iv) The $\Delta S°$ values for the ligand complexes are positive, confirming that the complex formation is entropically favorable [19].

An inspection of the results in Table 2 reveals that the pK^H values of ($\mathbf{HL_2}$) and its substituted derivatives are influenced by the inductive or mesmeric effect of the substituents. $\mathbf{HL_1}$ has a lower acidic character (higher pK^H values) than $\mathbf{HL_3}$. This is quite

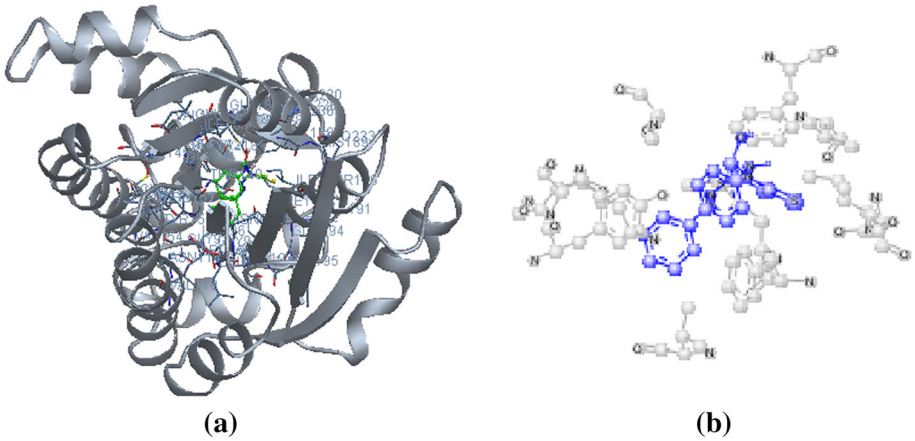

Fig. 6 The ligand ($\mathbf{HL_2}$) [*green* in (**a**) and *blue* in (**b**)] in interaction with receptor breast cancer mutant 3hb5. (For interpretation of the references to *color* in this figure legend, the reader is referred to the web version of this article.) (Color figure online)

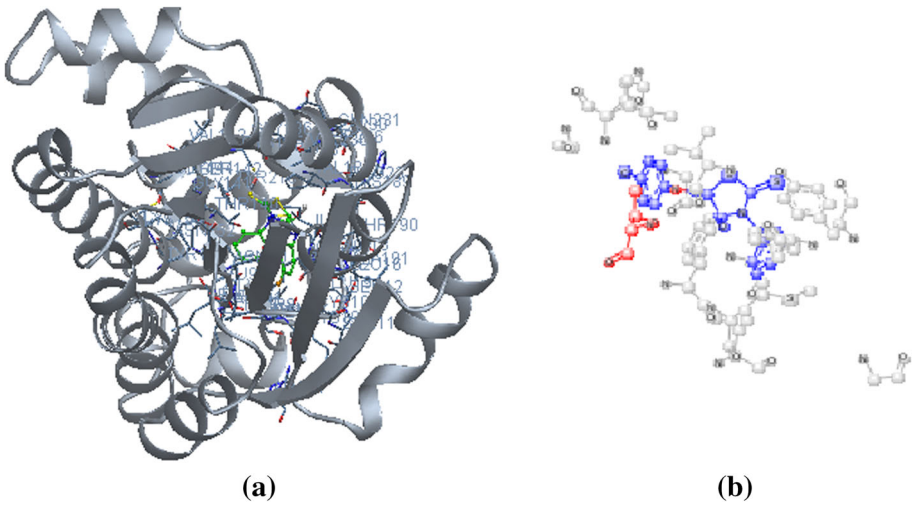

Fig. 7 The ligand ($\mathbf{HL_3}$) [*green* in (**a**) and *blue* in (**b**)] in interaction with receptor breast cancer mutant 3hb5. (For interpretation of the references to color in this figure legend, the reader is referred to the web version of this article.) (Color figure online)

reasonable because the presence of a *p*-CH_3 group (i.e. an electron-donating effect) will enhance the electron density by their high positive inductive or mesomeric effect, whereby a stronger O–H bond is formed. The presence of a *p*-Cl group (i.e. an electron-withdrawing

Table 5 Energy values obtained in docking calculations of ligands ($\mathbf{HL}_n$) with receptor breast cancer mutant 3hb5

Compound	Gibbs energy of binding ($kJ \cdot mol^{-1}$)	Inhibition constant (K_i) ($\mu mol \cdot dm^{-3}$)	vdW + H bond + desolve energy ($kJ \cdot mol^{-1}$)	Electrostatic energy ($kJ \cdot mol^{-1}$)	Total intermolecular energy ($kJ \cdot mol^{-1}$)	Surface interaction
$\mathbf{HL_1}$	−34.14	1.05	−39.87	−0.29	−40.1664	917.30
$\mathbf{HL_2}$	−32.55	1.98	−37.15	−0.08	−37.2376	782.03
$\mathbf{HL_3}$	−29.28	7.45	−35.48	0.12	−35.3548	841.02

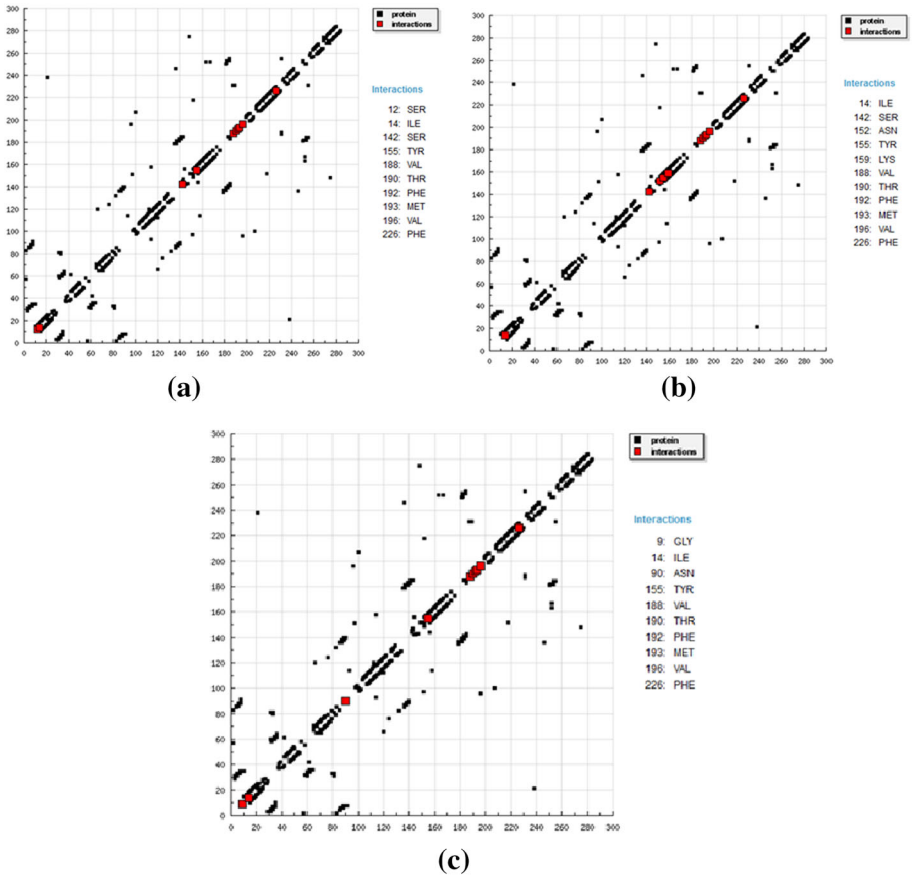

Fig. 8 HB plot of interaction between ligands **a** $\mathbf{HL_1}$, **b** $\mathbf{HL_2}$ and **c** $\mathbf{HL_3}$ with receptor breast cancer mutant 3hb5

effect) will lead to the opposite effect [47]. The results are also in accordance with Hammett's *para*-substituent constant values σ^R. Straight lines are obtained on plotting pK^H values at different temperature versus σ^R as shown in Fig. 4.

3.3 Molecular Docking

Molecular docking is a key tool in computer drug design [48]. The focus of molecular docking is to simulate the molecular recognition process. Molecular docking aims to achieve an optimized conformation for both the protein and drug with relative orientation between them such that the Gibbs energy of the overall system is minimized.

In this work, we used molecular docking between ligands ($\mathbf{HL}_n$) and breast cancer (3hb5). The results showed a possible arrangement between ligands ($\mathbf{HL}_n$) and receptor 3hb5. The docking study showed a favorable interaction between ligands ($\mathbf{HL}_n$) and the receptor 3hb5 as shown in Figs. 5, 6, and 7 and the calculated energy is listed in Table 5.

Table 6 Decomposed interaction energies of ligands $\mathbf{HL}_n$ with receptor breast cancer mutant 3hb5

	Hydrogen bonds	Polar	Halogen-bond	Cation-pi	Hydrophobic	Other
$\mathbf{HL}_1$	VAL188 (−0.659)	THR190 (−0.7525)		PHE226 (−0.3699)	PHE192 (−2.5937)	SER12 (−0.3769)
					TYR155 (−0.8648)	SER142 (−0.2248)
					ILE14 (−0.74)	
					MET193 (−0.5743)	
					VAL196 (−0.2553)	
$\mathbf{HL}_2$					PHE192 (−1.6761)	VAL196 (−0.6767)
					TYR155 (−1.2665)	MET193 (−0.4839)
					PHE226 (−0.4911)	SER142 (−0.3868)
					VAL196 (−0.3982)	ILE14 (−0.3508)
						LYS159 (−0.2634)
						ASN152 (−0.2148)
						THR190 (−0.2019)
$\mathbf{HL}_3$	THR190 (−0.7037)		ASN90 (−0.4185)	PHE192 (−1.3762)	TYR155 (−1.0834)	MET193 (−0.632)
			GLY9 (−0.1193)	PHE226 (−0.4002)	ILE14 (−0.6416)	
					VAL188 (−0.5677)	
					VAL196 (−0.1405)	

According to the results obtained in this study, the HB plot curve indicates that the ligands (**HL*n***) bind to the protein with hydrogen bonding interactions. The decomposed interaction energies, in kJ·mol^{-1}, between ligands (**HL*n***) with the 3hb5 receptor are shown in Fig. 8 and Table 6. The calculation efficiency is favorable where K_i values estimated by Auto-Dock were compared with experimental K_i values, when available, and the Gibbs energy change is negative. Also, based on this data, we can propose that interaction between the 3hp5 receptors and the ligands (**HL*n***) is possible; 2D curves of docking with ligands (**HL*n***) are shown in Fig. 9a–c. This interaction could activate apoptosis in cancer cells. Binding energies are most widely used as mode of measuring binding affinity of compounds. Thus,

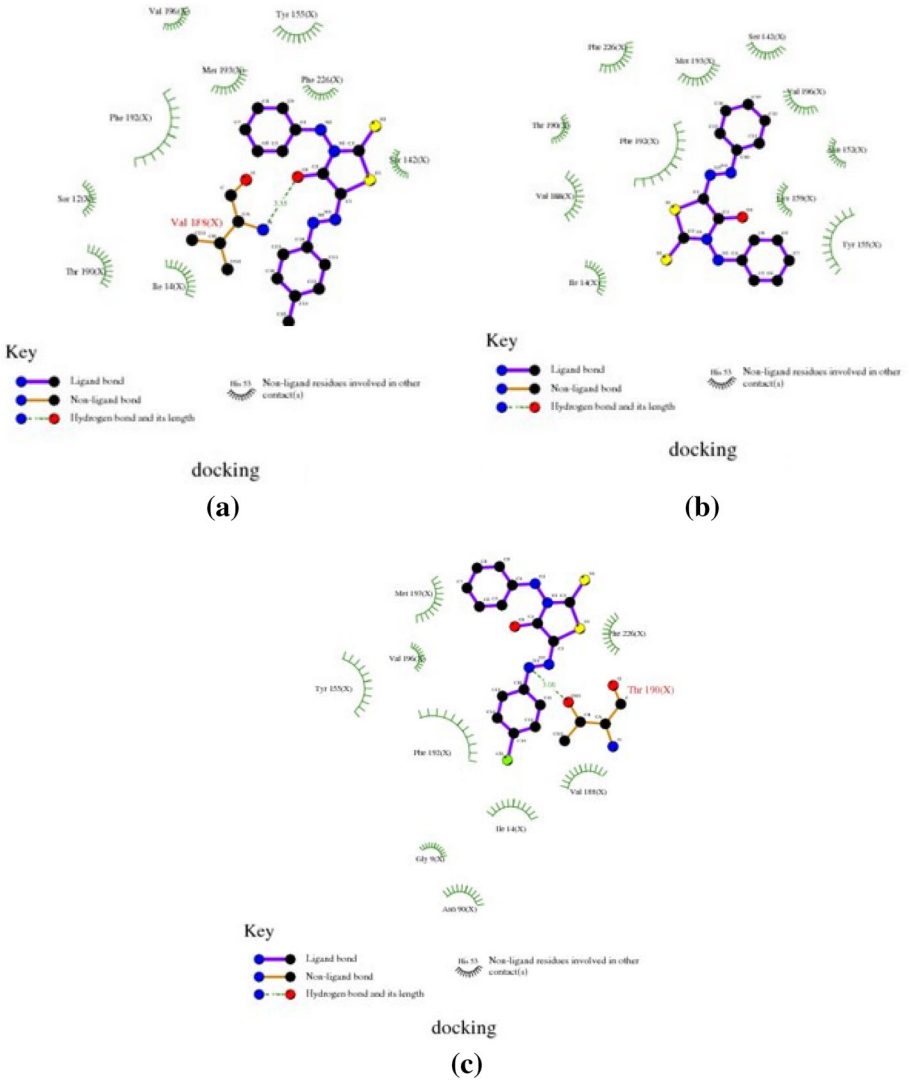

Fig. 9 2D plot of interaction between ligands **a HL$_1$**, **b HL$_2$** and **c HL$_3$** with receptor breast cancer mutant 3hb5

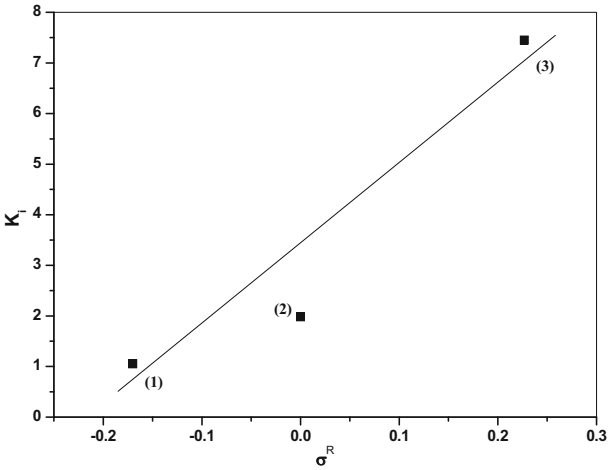

Fig. 10 The relation between Hammett's substitution coefficient (σ^R) and K_i of ligands ($\mathbf{HL}_n$)

the decrease in binding energy due to mutation will increase the binding affinity of the compounds towards the receptor. The characteristic features of compounds were represented in the presence of active sites available for hydrogen bonding. This feature gives them the ability to be good binding inhibitors to the protein and will help in the development of augmented inhibitory compounds. As shown in Table 5, the values of K_i are related to the nature of the para substituent, increasing in the order *p*-(Cl > H > CH_3). This can be attributed to the fact that the effective charge increases due to the electron withdrawing *p*-substituent $\mathbf{HL_3}$ while it is decreased by the electron donating character of $\mathbf{HL_1}$. This is in accordance with that expected from Hammett's constant (σ^R), and as shown in Fig. 10, the K_i values correlate with σ^R increasing with increasing σ^R. The results confirm also that the ligands derived from azo rhodanine derivatives ($\mathbf{HL}_n$) are efficient inhibitors of 3hb5-oxidoreductase breast cancer. The ligands ($\mathbf{HL_{1-3}}$) showed binding energies of −34.14, −32.55 and −29.28 kJ·mol^{-1}, respectively, with 3hb5-oxidoreductase breast cancer using H-bond, electrostatic and van der Waals interactions. On the basis of complex scoring and interactions with the active site residue and binding ability, it was shown that ligands ($\mathbf{HL}_n$) could be promising inhibitors of 3hb5-oxidoreductase breast cancer. This gives us the conclusion that $\mathbf{HL_1}$ possesses the lowest binding energy (−34.14 kJ·mol) and highest binding ability [49].

4 Conclusion

(1) 5-(4′-Alkylphenylazo)-3-phenylamino-2-thioxothiazolidin-4-one ($\mathbf{HL}_n$) compounds have been synthesized and characterized by different spectroscopic techniques.
(2) The proton–ligand dissociation constant of ligands ($\mathbf{HL}_n$) and metal–ligand stability constants of their complexes with metal ions Mn^{2+}, Co^{2+}, Ni^{2+} and Cu^{2+} were determined at different temperatures.
(3) The stability constants of the formed complexes increase with the order $Mn^{2+} < Co^{2+} < Ni^{2+} < Cu^{2+}$.
(4) The dissociation process is non-spontaneous, endothermic and entropically unfavorable.

(5) The formation of the metal complexes has been found to be spontaneous, endothermic and entropically favorable.
(6) The stability constants ($\log_{10} K_1$ and $\log_{10} K_2$) for the complexes increase with increasing temperature.
(7) The pK^H values of the ligands decrease in the order of $\mathbf{HL_1} > \mathbf{HL_2} > \mathbf{HL_3}$ as expected from Hammett's constant (σ^R).
(8) Molecular docking and binding energy calculations of azo dye ligands with the receptor of 3hb5-oxidoreductase breast cancer indicated that the present azo dye rhodanine ligands are efficient inhibitors of 3hb5-oxidoreductase breast cancer.
(9) The values of binding constant (K_i) of the ligands increase in the order $\mathbf{HL_1} < \mathbf{HL_2} < \mathbf{HL_3}$ as expected from Hammett's constant.

References

1. Martell, A.E., Motekaities, R.J.: The Determination and Use of Stability Constant, 2nd edn. VCH Publishers, New York (1992)
2. Bell, C.F.: Principles and Application of Metal Chelation. Oxford University Press, Oxford (1977)
3. Abou-Dobara, M.I., El-Sonbati, A.Z., Morgan, ShM: Influence of substituent effects on spectroscopic properties and antimicrobial activity of 5-(4′-substituted phenylazo)- 2-thioxothiazolidinone derivatives. World J. Microbiol. Biotechnol. **29**, 119–126 (2013)
4. Alegaon, S.G., Alagawadi, K.R., Sonkusare, P.V., Chaudhary, S.M., Dadwe, D.H., Shah, A.S.: Novel imidazo[2,1-b][1,3,4]thiadiazole carrying rhodanine-3-acetic acid as potential antitubercular agents. Bioorg. Med. Chem. Lett. **22**, 1917–1921 (2012)
5. Johnson, S.L., Chen, L.H., Harbach, R., Sabet, M., Savinov, A., Cotton, N.J., Strongin, A., Guiney, D., Pellecchia, M.: Rhodanine derivatives as selective protease inhibitors against bacterial toxins. Chem. Biol. Drug Des. **71**, 131–139 (2008)
6. El-Sonbati, A.Z., Belal, A.A.M., El-Gharib, M.S., Morgan, ShM: Supramolecular structure, mixed ligands and substituents effect on the spectral studies of oxovanadium(IV) complexes of bioinorganic and medicinal relevance. Spectrochim. Acta. A **95**, 627–636 (2012)
7. El-Sonbati, A.Z., Belal, A.A.M., Abd El-Meksoud, S.A., El-Boz, R.A.: Supramolecular structure, stereochemistry and substituents effect on the spectral studies of novel ruthenium complexes. J. Mol. Struct. **1027**, 200–206 (2012)
8. El-Sonbati, A.Z., Diab, M.A., Belal, A.A.M., Morgan, Sh.M.: Supramolecular structure and spectral studies on mixed-ligand complexes derived from b-diketone with azodye rhodanine derivatives. Spectrochim. Acta A **99**, 353–360 (2012)
9. Villain-Guillot, P., Gualtieri, M., Bastide, L., Roquet, F., Martinez, J., Amblard, M., Pugniere, M., Leonetti, J.P.: Structure-activity relationships of phenyl-furanyl-rhodanines as inhibitors of RNA polymerase with antibacterial activity on biofilms. J. Med. Chem. **50**, 4195–4204 (2007)
10. El-Sonbati, A.Z., El-Bindary, A.A., El-Dissouky, A., El-Gogary, T.M., Hilali, A.S.: Substituents effect on the spectral studies on rutheninum(III) complexes of 5(-4′-derivatives phenyldiazo)-3-phenyl-2-thioxo-4-thiazolidinone. Spectrochim. Acta A **58**, 1623–1629 (2002)
11. Zamani, H.A., Rajabzadeh, G., Ganjali, M.R.: Construction of a novel potentiometric terbium(III) membrane sensor and its application for the determination of terbium ion in binary mixture and fluoride ion in a mouth wash preparation. J. Braz. Chem. Soc. **17**, 1297–1303 (2006)
12. Rey-Castro, C., Castro-Vavela, R., Herrero, R., de Vicente, M.E.S.: Acid–base equilibria of phthalic acid in saline media: ion association from Pitzer equations. Talanta **60**, 93–101 (2003)
13. El-Sonbati, A.Z., Diab, M.A., El-Bindary, A.A., Morgan, ShM: Supramolecular spectroscopic and thermal studies of azodye complexes. Spectrochim. Acta A **127**, 310–328 (2014)
14. El-Ghamaz, N.A., El-Sonbati, A.Z., Diab, M.A., El-Bindary, A.A., Awad, M.K., Morgan, ShM: Dielectrical, conduction mechanism and thermal properties of rhodanine azodyes Mat. Sci. Semicon. Process. **19**, 150–162 (2014)
15. El-Sonbati, A.Z., Shoair, A.F., El-Bindary, A.A., Diab, M.A., Mohamed, A.S.: Synthesis, characterization, DNA binding and catalytic activities of Ru(III) complexes. J. Mol. Liq. **209**, 635–647 (2015)
16. Benson, J.R., Jatoi, I.: The global breast cancer burden. Future Oncol. **8**, 697–702 (2012)

17. Bates, R.G., Paabo, M., Robinson, R.A.: Interpretation of pH measurements in alcohol–water solvents. J. Phys. Chem. **67**, 833–1838 (1963)
18. Irving, H.M., Miles, M.G., Pettit, L.D.: A study of some problems in determining the stoicheiometric proton dissociation constants of complexes by potentiometric titrations using a glass electrode. Anal. Chim. Acta **38**, 475–488 (1967)
19. Bikadi, Z., Hazai, E.: Application of the PM6 semi-empirical method to modeling proteins enhances docking accuracy of AutoDock. J. Chem. Inf. **11**, 1–15 (2009)
20. Halgren, T.A.: Merck molecular force field. I. Basis, form, scope, parameterization, and performance of MMFF94. J. Computat. Chem. **17**, 490–519 (1998)
21. Morris, G.M., Goodsell, D.S., Halliday, R.S., Huey, R., Hart, W.E., Belew, R.K., Olson, A.J.: Automated docking using a Lamarckian genetic algorithm and empirical binding free energy function. J. Comput. Chem. **19**, 1639–1662 (1998)
22. El-Sonbati, A.Z., Diab, M.A., El-Bindary, A.A., Ghoneim, M.M., Mohesien, M.T., Abd El-Kader, M.K.: Polymeric complexes–LXI. Supramolecular structure, thermal properties, SS–DNA binding activity and antimicrobial activities of polymeric complexes of rhodanine hydrazone compounds. J. Mol. Liq. **215**, 711–739 (2016)
23. Jeffery, G.H., Bassett, J., Mendham, J., Deney, R.C.: Vogel's Textbook of Quantitative Chemical Analysis, 5th edn. Longman, London (1989)
24. Shoair, A.F., El-Bindary, A.A., El-Sonbati, A.Z., Beshry, N.M.: Molecular docking, potentiometric and thermodynamic studies of some azo quinoline compounds. J. Mol. Liq. **215**, 740–748 (2016)
25. El-Bindary, A.A., El-Sonbati, A.Z., Diab, M.A., Morgan, ShM: Geometrical structure, potentiometric and thermodynamic studies of rhodanine azodye and its metal complexes. J. Mol. Liq. **201**, 36–42 (2015)
26. El-Sonbati, A.Z., Mohamed, G.G., El-Bindary, A.A., Hassan, W.M.I., Elkholy, A.K.: Geometrical structure, molecular docking, potentiometric and thermodynamic studies of 3-aminophenol azodye and its metal complexes. J. Mol. Liq. **209**, 625–634 (2015)
27. El-Bindary, A.A., Hussein, M.A., El-Boz, R.A.: Molecular docking, theoretical calculations and potentiometric studies of some azo phenols. J. Mol. Liq. **211**, 256–267 (2015)
28. Irving, H., Rossotti, H.S.: The calculation of formation curves of metal complexes from pH titration curves in mixed solvents. J. Chem. Soc. **1954**, 2904–2910 (1954)
29. Farkas, E., Csoka, H.: Solution equilibrium studies on metal complexes of 2,3-dihydroxy-phenylalanine-hydroxamic acid (Dopaha) and models: catecholate versus hydroxamate coordination in iron(III)–, aluminium(III)– and molybdenum(VI)–Dopaha complexes. J. Inorg. Biochem. **89**, 219–226 (2002)
30. Omar, M.M., Mohamed, G.G.: Potentiometric, spectroscopic and thermal studies on the metal chelates of 1-(2-thiazolylazo)-2-naphthalenol. Spectrochim. Acta A **61**, 929–936 (2005)
31. Irving, H., Rossotti, H.S.: Methods for computing successive stability constants from experimental formation curves. J. Chem. Soc. **47**, 3397–3405 (1953)
32. Rossotti, F.J.C., Rossotti, H.S.: Graphical methods for determining equilibrium constants. Acta Chem. Scand. **9**, 1166–1176 (1955)
33. Beck, M.T., Nagybal, I.: Chemistry of Complex Equilibrium. Wiley, New York (1990)
34. Khalil, M.M., Radalla, A.M., Mohamed, A.G.: Potentiometric investigation on complexation of divalent transition metal ions with some zwitterionic buffers and triazoles. J. Chem. Eng. Data **52**, 3261–3272 (2009)
35. Soayed, A.A., El-Husseiny, A.F.: Potentiometry and geometrical structure of some azodye compounds and their metal complexes. J. Mol. Liq. **209**, 258–266 (2015)
36. Sridhar, S., Kulanthaipandi, P., Thillaiarasu, P., Thanikachalam, V., Manikandan, G.: Protonating and chelating efficiencies of some biologically important thiocarbonohydrazides in 60%(v/v) ethanol–water system by potentiometric and spectrophotometric methods. J. Chem. **4**, 133–140 (2009)
37. Athawale, V.D., Lele, V.: Stability constants and thermodynamic parameters of complexes of lanthanide ions and (±)-norvaline. J. Chem. Eng. Data **41**, 1015–1019 (1996)
38. Athawale, V.D., Nerkar, S.S.: Stability constants of complexes of divalent and rare earth metals with substituted salicynals. Monatsh. Für Chem. **131**, 267–276 (2000)
39. Mohamed, G.C., Omar, M.M., Ibrahim, A.: Biological activity studies on metal complexes of novel tridentate Schiff base ligand. Spectroscopic and thermal characterization. Eur. J. Med. Chem. **44**, 4801–4812 (2009)
40. Ibañez, G.A., Escandar, G.M.: Complexation of cobalt(II), nickel(II), and zinc(II) ions with mono and binucleating azo compounds: a potentiometric and spectroscopic study in aqueous solution. Polyhedron **17**, 4433–4441 (1998)
41. Malik, W.U., Tuli, G.D., Madan, R.D.: Selected Topics in Inorganic Chemistry, 3rd edn. Chand S. and Co. LTD, New Delhi (1984)

42. Harlly, F.R., Burgess, R.M., Alcock, R.M.: Solution Equilibria, p. 257. Ellis Harwood, Chichester (1980)
43. Orgel, L.E.: An Introduction to Transition Metal Chemistry Ligand Field Theory, p. 55. Methuen, London (1966)
44. Bebot-Bringaud, A., Dange, C., Fauconnier, N., Gerard, C.: 31P NMR, potentiometric and spectrophotometric studies of phytic acid ionization and complexation properties toward Co^{2+}, Ni^{2+}, Cu^{2+}, Zn^{2+} and Cd^{2+}. J. Inorg. Biochem. **75**, 71–78 (1999)
45. Al-Sarawy, A.A., El-Bindary, A.A., El-Sonbati, A.Z., Omar, T.Y.: Potentiometric and thermodynamic studies of 3-(4-methoxyphenyl)-5-azorhodanine derivatives and their metal complexes with some transition metals. XIV. Chem Pap. **59**, 261–266 (2005)
46. Mubarak, A.T., El-Sonbati, A.Z., El-Bindary, A.A.: Potentiometric and conductometric studies on the complexes of some transition metals with rhodanine azosulfonamide derivatives. XI. Chem. Pap. **58**, 320–323 (2004)
47. El-Bindary, A.A., El-Sonbati, A.Z., Diab, M.A., El-Katori, E.E., Seyam, H.A.: Potentiometric and thermodynamic studies of some Schiff-base derivatives of 4-aminoantipyrine and their metal complexes. Int. J. Adv. Res. **2**, 493–502 (2014)
48. Lulu, A.S.S., Thabitha, A., Vino, S., Priya, A.M., Rout, M.: Naringenin and quercetin: potential anti-HCV agents for NS2 protease targets. Nat. Prod. Res. **30**, 464–468 (2016)
49. Beteringhe, A., Racuciu, C., Balan, C., Stoican, E., Patron, L.: Molecular docking studies involving transitional metal complexes (Zn(II), Co(II), Cu(II), Fe(II), Ni(II) with cholic acid (AC) as ligand against Aurora A kinase. Adv. Mater. Res. **787**, 236–240 (2013)